Title: Growth Kinetics in Layer-by-Layer Assemblies of Organic Nanoparticles and Polyelectrolytes

Authors: Maziar Mohammadi, M.Sc. in Mechanical Engineering; Ali Salehi, M.Sc. in Chemical Engineering; Ryan J Branch; Lucas J Cygan; Cagri G Besirli, M.D., Ph.D.; Ronald G. Larson, Ph.D. in Chemical Engineering

To be cited as: ChemPhysChem 10.1002/cphc.201600789

Link to VoR: https://doi.org/10.1002/cphc.201600789

Growth Kinetics in Layer-by-Layer Assemblies of Organic Nanoparticles and Polyelectrolytes

Maziar Mohammadi,[a] Ali Salehi,[b] Ryan J. Branch,[b] Lucas J. Cygan,[b] Cagri G. Besirli,[c] and Ronald G. Larson*[a,b]

Abstract

We systematically measure the growth rate of layer-by-layer (LbL) assemblies of polyelectrolytes (PEs) with oppositely charged polystyrene (PS) nanoparticles (NPs) as a function of molecular weight (MW) of PEs, ionic strength of the media, and NP size and charge. To optimize the LbL growth, we assess the effects of suspension concentration, pH of the media, and deposition time on the growth rate of multilayers. Both linear and exponential growth behaviors are observed, and under optimal conditions films of up to around 1 μm thickness can readily be assembled after 10 or so bilayers have been deposited. For many of the cases studied, an intermediate MW of PE leads to the fastest film buildup, for both cationic poly(ethyleneimine) deposited alternately with anionic PS NPs and for anionic poly(acrylic acid) deposited alternately with cationic PS NPs. The existence of an optimal MW suggests that growth rate is determined by a balance of thermodynamic factors including density of polymer bridges between particles, and kinetic factors, specifically the diffusivity of polymer in the film. The optimal MW, however, is very sensitive to the materials used. Moreover, depending on the MW of the PE, increasing salinity could increase or decrease the growth kinetics. Finally, we characterize the surface morphology of the films with atomic force microscopy and scanning electron microscopy and find that the roughness increases less than linearly with film thickness.

1. Introduction

Functional thin films have attracted significant attention recently,[1, 2] due to their versatility and ease of fabrication. One of the most flexible methods of assembling these films is by layer-by-layer (LbL) deposition, which is the alternating deposition of oppositely charged polyelectrolytes (PEs) or oppositely charged PEs and nanoparticles (NPs). LBL assembled thin films are easy to fabricate, inexpensive, and their properties can be finely tuned.[3, 4] Furthermore, the process of making these films does not need to be done under extreme conditions.[5]

Even though the major driving force for the LbL

[a] M. Mohammadi, Prof. R.G. Larson
Department of Mechanical Engineering, University of Michigan, Ann Arbor, Michigan, 48109, USA.
Email: rlarson@umich.edu

[b] A. Salehi, R.J. Branch, L.J. Cygan, Prof. R.G. Larson
Department of Chemical Engineering, University of Michigan, Ann Arbor, Michigan, 48109, USA.

[c] Dr. C.G. Besirli
Department of Ophthalmology and Visual Sciences, Kellogg Eye Center, University of Michigan, Ann Arbor, Michigan, 48105, USA.

Supporting information for this article is given via a link at the end of the document.

assembly is usually electrostatic interactions, other interactions including hydrogen bonding, hydrophobic interactions, host-guest interactions, covalent bonding, etc., lead to the formation of such assemblies.[4, 6] In electrostatically driven PE/PE assembly, LbL growth occurs due to charge overcompensation, i.e. each film ingredient deposited on the surface reverses the surface charge, making it ready to adsorb the next LbL layer.[4] LbL assembly of PEs and organic NPs has considerable applications in drug delivery, coating, creation of three dimensional scaffolds, and sensors to name but a few.[4, 7-16] However, little is known about the mechanism of their growth, and its effective parameters. Thus, it is important to study PE/organic NP LbL films to better understand the effects of different parameters on their assembly and growth.

A major parameter affecting the growth kinetics of LbL films is the molecular weight (MW) of the PE. MW affects the diffusion of the PE chains within the PE matrix and their mobility in the bulk solution. Moreover, MW influences the thermodynamic driving force for the diffusion and the overall integrity of the LbL film. For PE/PE films, several studies have shown the dramatic effect of MW on the thickness and morphology.[17-20] Nestler et al. studied the effect of MW on the growth kinetics of poly(styrenesulfonate) (PSS hereafter)/ poly(diallyldimethylammonium chloride) (PDADMAC hereafter) multilayer films.[17] Below a certain MW, they demonstrated that an increase in the MW of the polyanion (PSS) decreases both the film thickness and the layer number at which the growth rate changes to the linear regime. However, they reported a completely opposite trend in response to a variation of the MW of the polycation (PDADMAC). Shen et al. studied the effect of the polyanion (hyaluronan) MW on the growth kinetics of poly(L-lysine)/hyaluronan LbL films.[18] In contrast to Nestler et al.,[17] they showed that increasing the polyanion MW increases the film thickness. This reveals the complex effect of MW of the PE on LbL growth and suggests that it depends on the specific system being studied.

In contrast to PE/PE films, very few studies have addressed the effect of MW of the PE on the growth kinetics and surface morphology of PE/NP films, and even for these, the MW was not the main focus. Rahman and Taghavinia used poly(ethyleneimine) (PEI) with two different MWs (1.3 and 750 kg/mol) to grow PEI/TiO_2 NP composites.[3] They measured LbL growth with UV-visible spectrophotometry and concluded that film growth is 25 % slower when PEI with the lower MW is employed. In another study by the same group, Rahman et al. showed greater deposition for PEI/TiO_2 NP composites with lower MW PEI.[21] They explained this opposite growth behavior by noting that the substrate and its geometry have important effects on the film growth. In the later study, they grew composites on cellulose fibers as opposed to the planar quartz sheets that they employed for the earlier work. They claimed that PEI with lower MW could diffuse into the porous structure of cellulose faster. In addition, they showed that films with lower MW of PEI have a less porous structure. In contrast to findings of Rahman et al.[3, 21] which showed a large effect of MW of PE on growth and structure of TiO_2 composites, Kniprath et al. illustrated that the surface characteristics of PSS/TiO_2 NP or PDADMAC/TiO_2 NP films are independent of the MW of the PE.[5] They used MWs of 70 kg/mol and 1,000 kg/mol for PSS and < 100 kg/mol and 400 to 500 kg/mol for PDADMAC. In these studies, only a couple of MWs were considered, so it is hard to reach a conclusive picture of the effect of MW. Thus,

there is need for further study of MW on the growth kinetics and surface morphology of PE/NP composite films.

In addition to the MW of the PE, the pH and salinity of the deposition solutions are decisive factors affecting the buildup of the LbL films. The pH, for example, affects the charge density of weak PEs.[22] Bieker and Schönhoff investigated the effect of the pH of the depositing solutions on the growth of poly(allyl amine hydrochloride) (PAH)/poly(acrylic acid) (PAA) LbL assemblies.[23] They discovered various growth regimes with different growth behavior (linear and exponential) and film quality (soft and rigid) with simple variation of pH. They rationalized their observations by noting that at different pH values, the degrees of ionization, electrostatic interactions, mobility and inter-diffusion of PE chains vary. Peng et al. studied the effect of pH and salinity of deposition solutions on the growth kinetics of PEI/SiO_2 NP composites, showing that deposition of low pH SiO_2 NPs and high pH PEI result in exponential film growth.[24] They claimed that the pH difference between PEI and SiO_2 solutions during the LbL assembly alters the charge of PEI chains and thereby enhances their diffusion, so that during a single nanoparticle deposition step, more nanoparticles are able to be deposited, leading to deposition of multiple layers of SiO_2 NPs in a single deposition step.

Salt has two competing effects on the growth kinetics of LbL films. First, simple ions screen the electrostatic interactions and reduce the driving force for LbL assembly.[22] Second, salt-induced weakening of electrostatic interactions increases the diffusivity of polymer chains and affects their conformation. Recently, our group studied the effect of pH and salinity on the growth of PE/PE LbL films and how the growth rate correlates to the bulk complexation thermodynamics of the two PEs at the same pH and salinity.[22] It was shown that even though there is no one-to-one correlation between different regimes of LbL growth (linear and exponential growth) and bulk complexation (precipitate and coacervate formation), salinity influences the growth kinetics in a more or less universal fashion. It was shown that growth rate increases with salinity at low salt concentration, while it decreases as the salt concentration approaches the critical concentration for dissolution of the bulk polymer-rich phase into a single-phase. It was demonstrated that depending on the PEs employed, variation of pH and salinity could dramatically alter the growth mode of LbL films from linear to exponential and vice versa.

The effects of ionic strength of the deposition media on the growth rate of PE/NP composites have been studied as well.[5, 24-28] Ghannoum et al. studying the growth kinetics of LbL assembly of PDADMAC and platinum NPs capped with poly(acrylate), showed that film growth is very sensitive to the ionic strength of the suspension.[25] They identified 50 mM as the optimum salt concentration beyond which film growth degrades. Some of the studies focused on the salinity of PE solutions, as the addition of salt to particulate suspensions could lead to aggregation as electrostatic repulsion is screened. Peng et al. demonstrated that addition of salt to a PEI solution degraded the growth of PEI/SiO_2 NP films.[24] In contrast, Ostendorf et al. reported that increasing the ionic strength of PAH solutions up to 1 M increases the thickness of PAH/gold NP films somewhat, although it did not seem

to affect the amount of NPs deposited in the film.[26] Kniprath et al., on the other hand, found that increasing the ionic strength of the PE solution from 0 to 1 M did not affect the surface morphology of the resulting PSS/TiO_2 NP or PDADMAC/TiO_2 NP films.[5] All in all, it seems that the only clear conclusion that can be drawn is that the effect of salinity on the growth and structure of LbL films strongly depends on the specific chemistry of the ingredients.

Despite the importance of the observations made in previous studies, to the best of our knowledge, there is no systematic study of the effect of the MW of the PE on the growth kinetics of PE/organic NP LbL films. We will therefore here elucidate how MW affects the way growth kinetics varies with NP size and salinity of the media (both PE and PS solutions). We also investigate the surface morphology of the LbL films with different MWs using atomic force microscopy (AFM) and scanning electron microscopy (SEM). As a model for organic NPs, we choose polystyrene (PS) beads of different size and surface functionalization to study the growth kinetics of their LbL assembly with two different PEs, namely, PEI and PAA. Being weakly dissociating PEs, PEI and PAA are selected so that their charge density can be tuned with pH. Prior to studying the effect of MW, we examine the effect of the NP concentration, the pH of the deposition solutions, and the deposition time to find the optimal growth conditions for each parameter. This study is aimed at engineering the structure of LbL films composed of organic NPs and PEs.

2. Results and discussion

2.1. PEI/PS- system

Initially a multilayer system composed of positively charged PEI as the polyelectrolyte and negatively charged PS (PS- hereafter) NPs carrying strongly charged sulfate functional groups were chosen. The effects of deposition time, NP concentration, solution pH, and PEI MW on growth were studied. We will show that variation of these parameters enables us to tune the growth kinetics of PEI/PS- composites. Results for the effect of deposition time on film buildup are shown in the supporting information (Fig. S1) for brevity.

2.1.1. Effect of nanoparticle concentration

Figure 1 indicates the effect of NP concentration on the growth kinetics of a PEI/PS- composite.

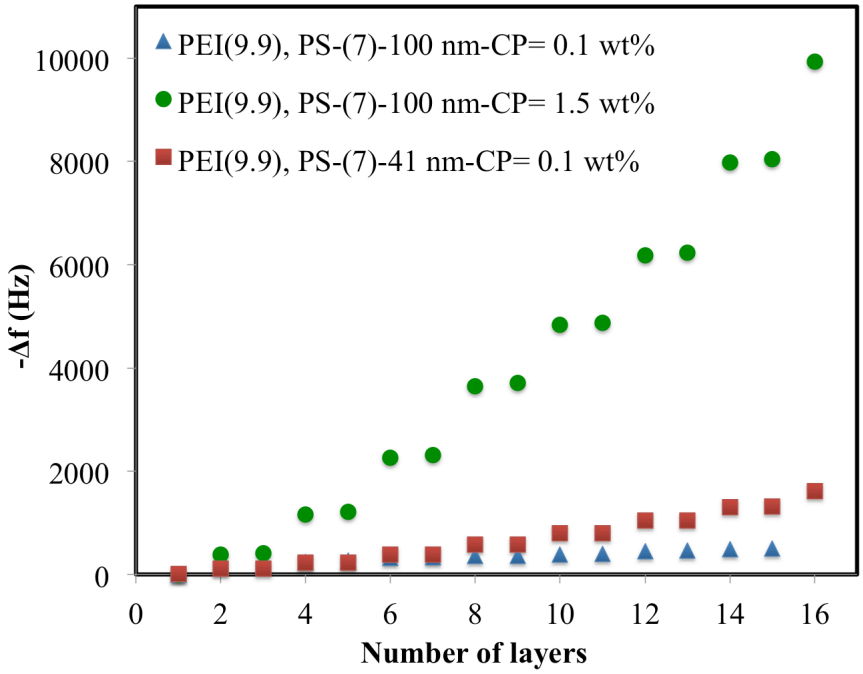

Figure 1. The effect of NP concentration and size on the growth kinetics of a PEI/PS- thin film. PS- NPs are deposited during the even-numbered steps. PEI with a MW of 750 kg/mol is used. In the legend, the numbers in the parentheses indicate the pH value of the solutions. For each case, the diameter of the employed NPs is given in nm in the figure legend. "CP" stands for concentration of particles. In this and all figures, the polymer monomer concentration used in the solutions is 0.23 M.

As shown in Fig. 1, for the same mass concentration of 0.1 wt%, smaller NPs (41 nm-sized ones) lead to larger frequency shifts and thus greater mass depositions in the PEI/PS- film, which may seem counter-intuitive. However, for the same mass concentration, larger NPs have a lower number density in the solution than do smaller ones. Due to their much slower diffusion, it is therefore less likely for the larger NPs to get adsorbed into the PEI/PS- composite.

To find the proper basis for assessing particle concentration, the growth of films with 100 nm-sized particles was studied at the same particle number density as that for 41 nm-sized ones. A dense suspension of 100 nm-sized particles with a concentration of 1.5 wt% (which has the same number density as a 0.1 wt% suspension of 41-nm particles) was therefore used in combination with a PEI solution of the same concentration as before to grow PEI/PS- multilayers. For this case, the deposition rate of PS- NPs was so fast that the entire chrome/gold crystal was instantly coated by a visibly thick layer of NPs. At the same number density, the larger 100 nm particle suspension produces an LbL film with a frequency shift that is at least five times greater than that of the smaller 41 nm-sized particles. Thus, there does not seem to be an obvious choice for a concentration basis at which composite films of different NP sizes yield the same growth rate. Consequently, for simplicity, the rest of the experiments are carried out with PS NPs of 0.1 wt% concentration. It is also evident from Fig. 1 that for

the same NP size of 100 nm, increasing the suspension concentration boosts the growth kinetics of PEI/PS- thin films.

Finally, the data of Fig. 1 indicates that PEI/PS- thin films grow through a cooperation between PEI and PS- deposition steps. The more PEI that is deposited in an LbL step, the more PS- NPs are deposited in the subsequent step. Also, the "stepped" appearance of the growth or "odd-even" effect in this figure, with a relatively small mass added in the odd steps, shows that contribution of the PEs to the frequency shift was much less than that of the NPs. This trend was observable for all growth study experiments. This phenomenon has already been reported in the literature.[28]

2.1.2. Effect of solution pH

Figure 2 depicts the influence of pH on the buildup of PEI/PS- multilayers. PS- NPs are functionalized with sulfate groups, so their surface charge is independent of pH and they are stable over a wide range of pH. On the other hand, PEI is a weak PE (pK_b~10 [24]) whose charge density is dependent on pH. At pH = 9.9, PEI should be nearly 50 % charged, while decreasing the pH to 7 renders PEI chains nearly fully charged. PS- NPs with a diameter of 41 nm were chosen, as their diameter was an intermediate value among the group of PS- NPs studied in this article.

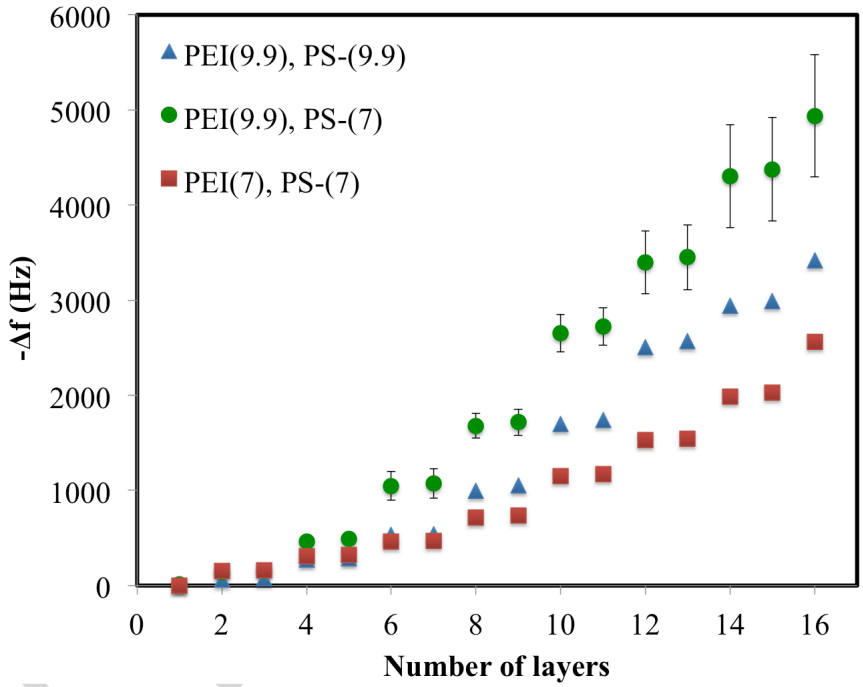

Figure 2. The effect of pH on LbL growth of a PEI/PS- composite. PEI with a MW of 70 kg/mol and 41 nm-sized PS- particles are employed. The concentration of PS- NPs is 0.1 wt%.

As shown in Fig. 2, the pH values of both the PEI solution and of the PS- suspension have considerable influence on the growth kinetics of the PEI/PS- composite. Furthermore, the growth rate of the PEI/PS- film is fastest when PEI and PS- solutions have pH values of 9.9 and 7, respectively.

The degree of ionization has a dramatic influence on the growth rate of a PEI/PS- composite. When PEI and negatively charged PS solutions are deposited at the same pH (= 7.0), PEI chains are

expected to be fully charged. When PEI chains are deposited at pH = 9.9, however, their charge is less than it is at pH = 7.0, and more chains need to deposit atop the underlying NPs to compensate the opposite charge on the film. Based on the pK_b of PEI in the bulk, the charge density of PEI at pH 7 should be roughly twice as high as it is at pH 9.9. It should be noted, however, that weakly dissociating PEs of oppositely charged functional groups inside PE/PE multilayer films have long been shown to be more highly charged than in solution via the charge regulation effect.[29, 30] The surface functional groups on PS- NPs can thus induce further charging in PEI chains at pH 9.9 once they are fully embedded in the film. However, since the growth is markedly faster for PEI chains depositing at pH 9.9 with PS- NPs at pH 7, as compared to the other two conditions studied in Fig. 2, the PEI chains depositing at pH 9.9 are likely far from being fully charged. Therefore, the PS- NPs need to absorb more PEI chains at pH 9.9 than they do at pH 7 to achieve charge compensation, leading to faster growth.

The degrees of charge compensation for three different LbL growth experiments studied in this section are presented in the supporting information (Fig. S2). From the QCM data shown in Fig. 2, we understand that the frequency shift ratio (or equivalently the mass per unit area ratio) of deposited NPs to that of PEs in each double layer is on the order of 10, while the charge compensation factor (defined as the ratio of charges associated with NPs to those of PEs) for each double layer for these experiments is on the order of only 0.01 (see Fig. S2 in the supporting information), indicating that the charges on the NP's deposited in a layer fall far below that needed to compensate the charge on the PE layer deposited in the layer just beneath it. (We must here add the important caveat that the difference in total film mass between deposition of each layer is taken as a measure of the mass actually deposited from the solution. It is possible that mass of NP's deposited is much greater than this, if an equivalent mass of PE is washed off the film as the NP's are deposited.) The lack of strong charge regulation can thus be rationalized by fewer encounters between neutral PEI repeat units with particle surface functional groups in PE/NP films than would be expected in PE/PE films assembled under similar conditions. The NPs evidently serve as a sufficiently thick spacer between two alternating PEI layers that render a continuous film build-up feasible despite the very low charge compensation ratios observed. Such excess of charge on PE chains in conventional PE/PE LbL assembly is unsustainable owing to a huge electrostatic repulsion that would be created between narrowly spaced layers of PE present in excess. Evidently, in PE/NP deposition, accumulation of PE charge from one bilayer to the next is possible. This is an unusual feature that to our knowledge is unique to PE/NP assemblies.

Upon deposition of NPs at pH = 7 following PEI deposition at pH = 9.9, the neutral primary amine groups absorb a proton from the solution as a result of the sudden pH drop, thus creating a sudden jump in areal charge density of the chains decorating the surface. The higher charge density of the PEI-covered surface requires more sulfate-functionalized PS NPs to compensate, as compared to the

cases without the abrupt pH change. Consistently, PEI and PS- NPs deposited at the same pH, either both at 7 or both at 9.9, yield thinner films than when the solutions are deposited at the two different pH values considered (Fig. 2). Such a sudden charging of PEI chains is lacking when the solutions are deposited at the same pH.

Moreover, the film growth benefits from the high diffusivity of PEI chains into the film during the PEI deposition at pH = 9.9 due to lower charge density of PEI chains, which should lead to weaker binding to PS- particles, and hence faster diffusion.[22] The higher diffusivity of PEI chains at pH = 9.9 is probably another reason for the faster growth kinetics of PEI/PS- composite at this pH compared to the case where both solutions are deposited at a pH of 7, despite the stronger electrostatic interactions in the latter case.

As discussed in the experimental section, the pH of the rinsing water and of the PS NP suspension drift during the deposition. The result is that when the PS particles and PE polymer are deposited at different pH values, nominally pH = 7 for PS- and nominally pH = 9.9 for PEI, the actual pH values differ less from each other as more layers are deposited. As shown in the supporting information (Fig. S3), when the pH values of the rinsing water and of the PS- suspension were constantly monitored and maintained at their initial values, the film growth was improved. This observation further bolsters our argument that larger difference between pH values of deposition solutions and rinsing waters leads to faster LbL film buildup.

The effect of pH on the growth kinetics of PEI/PS- composites observed here is similar to that observed by Peng et al. for the multilayer buildup of SiO_2 inorganic NPs and PEI.[24] Here, we have shown that even though the interactions are not exactly the same, a similar trend holds.

2.1.3. Effect of molecular weight

Figures 3-5 indicate the role of PEI MW on the growth kinetics of PEI/PS- composites for different NP sizes. The NP concentration is set to 0.1 wt%.

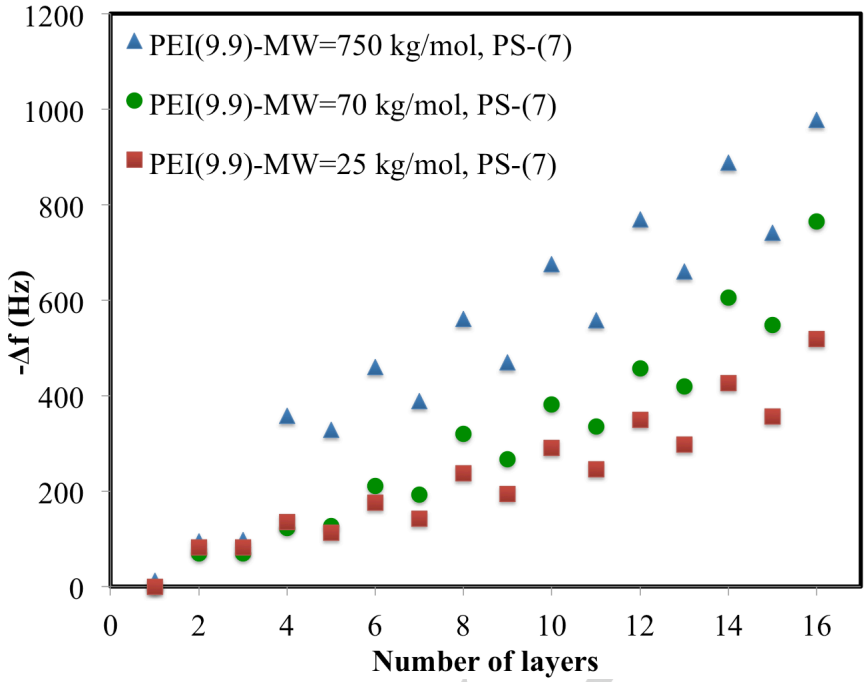

Figure 3. The role of MW of PEI on growth of PEI/PS- LbL film, for PS- NP size of 26 nm.

Conspicuous in Fig. 3 is the saw-tooth growth behavior of the films involving the 26 nm PS- particles. It seems that some of the deposited PS- NPs are washed off of the film during the deposition of the PEI (odd numbered steps). Some PEI must have been deposited during these steps to explain the continued growth of the film in the subsequent steps. Moreover, Fig. 3 indicates that for 26-nm PS- particles, a higher MW of 750 kg/mol leads to a thicker PEI/PS- composite.

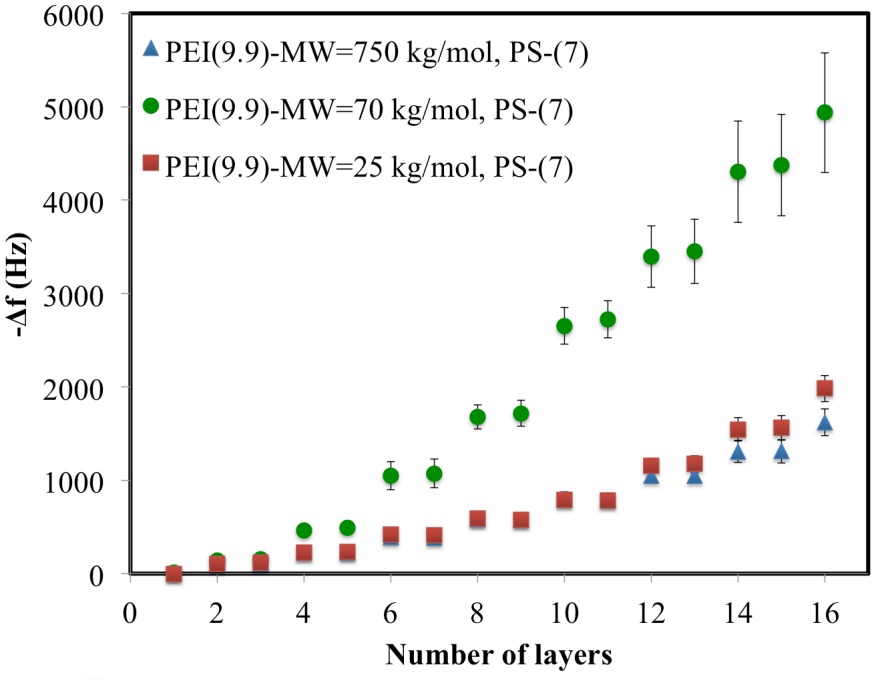

Figure 4. The same as Fig. 3, except for a particle size of 41 nm.

Figure 4 shows that for the 41 nm PS- particles, the PEI/PS- LbL buildup is maximum at an intermediate PEI MW of 70 kg/mol. Also, unlike the growth kinetics of the 26 nm-sized PS- particles, for 41 nm-sized PS- particles, out-diffusion of ingredients from the film is not observed. Moreover, all three data sets depicted in Fig. 4 show accelerating, or "exponential" growth for the particle deposition steps, with increasing numbers of layers. This is especially noticeable for the PEI with a MW of 70 kg/mol.

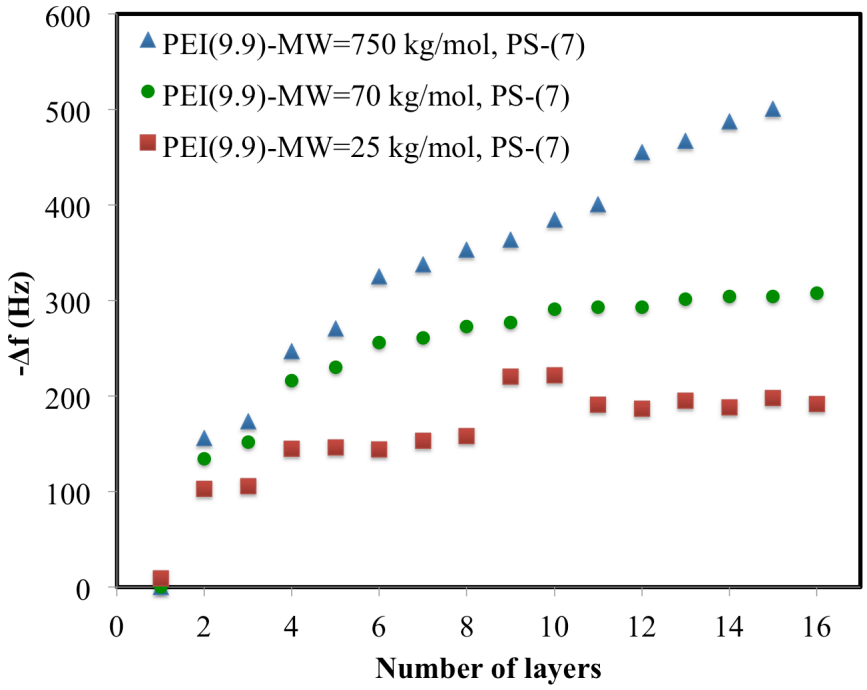

Figure 5. The same as Fig. 3, for particle size of 100 nm.

According to Fig. 5, for 100 nm-sized PS- particles, the PEI with the highest MW leads to the thickest film.

2.2. PAA/PS+ system

In the next set of experiments, another composite system composed of negatively charged PAA as the PE and positively charged PS (PS+ hereafter) NPs carrying amidine functional groups was selected. PAA is a weak PE (pK_a of around 5-5.5 [22]). It is approximately 50 % charged at pH = 5, and therefore almost completely charged at a pH of 7.

If the PE/NP LbL growth were entirely driven by electrostatic interactions, it would be plausible to expect that switching the sign of charges on both components should not alter the trends. The LbL experiments with PAA/PS+(amidine) system will thus establish whether the trends observed for the effect of MW on the growth of PEI/PS-(sulfate) multilayers discussed in the previous section are general, i.e. chemistry-independent. Similar to the PEI/PS- system, for the PAA/PS+ composite,

increasing the PS+ concentration boosts the growth rate, as shown in the supporting information (Fig. S4).

2.2.1. Effect of molecular weight

Figures 6-8 show the growth kinetics of PAA/PS+ LbL assemblies for different MWs of PAA and various NP sizes. Throughout this section, concentration of PS+ NPs was set to 0.1 wt%.

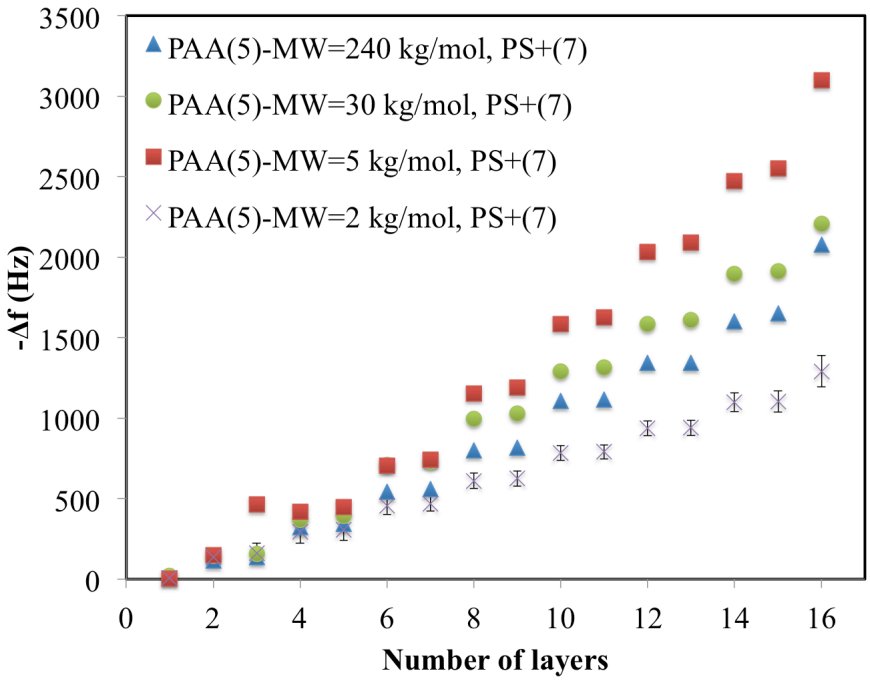

Figure 6. Effect of MW of PAA on PAA/PS+ LbL buildup with 23 nm-sized PS+ particles. For this and subsequent figures, the pH values for each deposition solution (PAA or PS+) is indicated in parenthesis in the figure legend. Note the small value of error bars for PAA with MW of 2 kg/mol.

Unlike the PEI/PS- system with 26 nm-sized particles (Fig. 3), out-diffusion of the PS+ NPs of similar size, 23 nm, is not observed for the PAA/PS+ counterpart shown in Fig. 6.

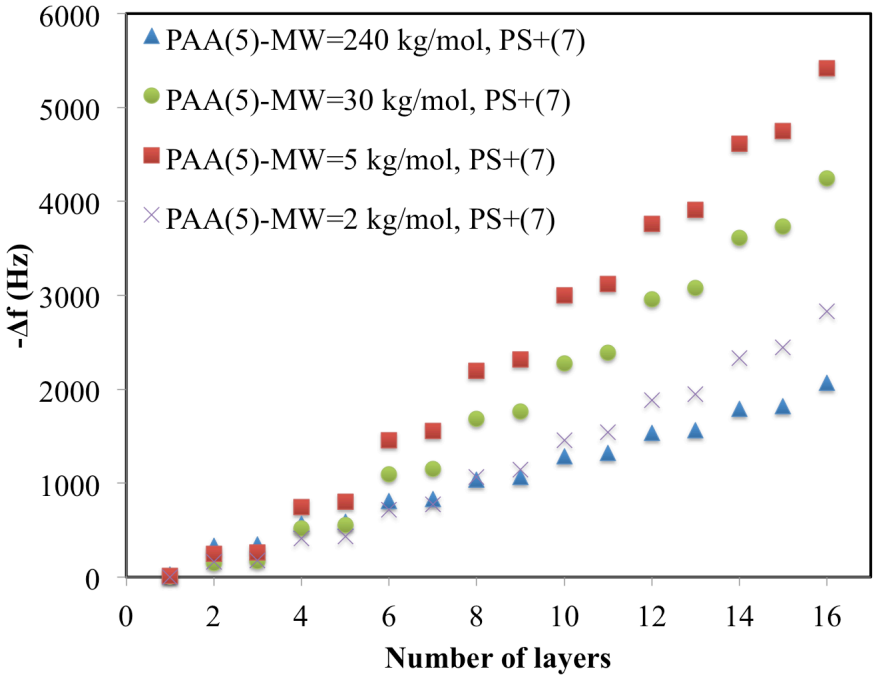

Figure 7. The same as Fig. 6, for 44 nm-sized PS+ particles. Data for PAA with a MW of 30 kg/mol have error bars, but these are too small to be visible.

According to Figs. 6 and 7, the MW has a non-monotonic effect on the LbL buildup of PS+ particle of sizes 23 and 44 nm. Decreasing the MW from 240 to 5 kg/mol boosts the LbL growth rate, but a further decrease in MW leads to a slower growth rate. Evidently a further decrease in the MW to 2 kg/mol lowers the capability of chains to immobilize the PS+ NPs in the composite film. Therefore, there is an optimum MW for the growth of PAA/PS+ multilayers, which is 5 kg/mol for both 23 and 44 nm-sized PS+ particles.

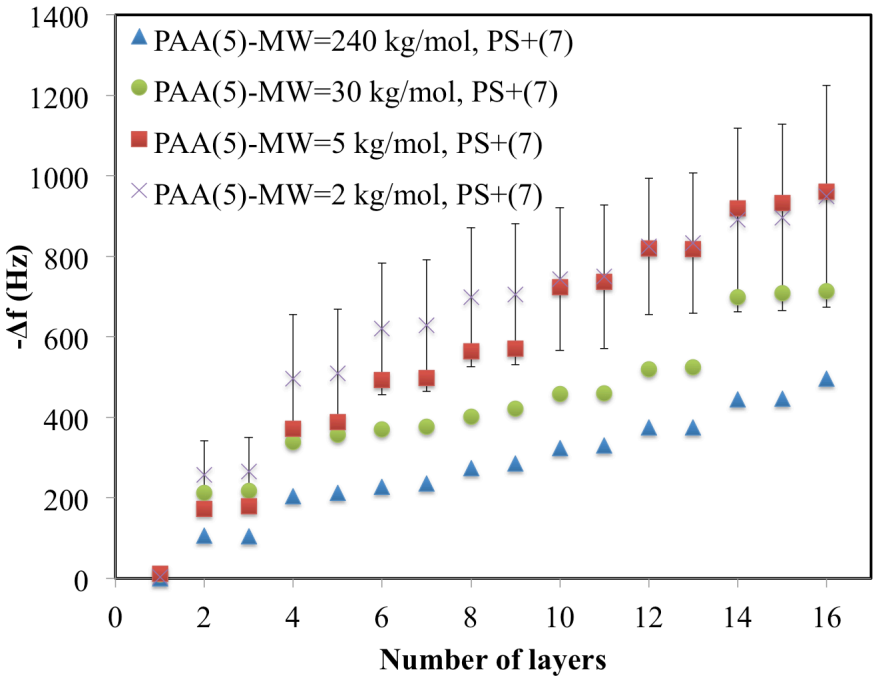

Figure 8. The same as Fig. 6, for 100 nm-sized PS+ particles.

Given the margin of error in Fig. 8, however, the growth of PAA and 100 nm-sized NP film is virtually insensitive to a further decrease of MW from 5 to 2 kg/mol. We speculate that, similar to behavior of the PS+ NPs of sizes 23 and 44 nm, for 100-nm particles there should be an intermediate MW that leads to the fastest growth of PAA/PS+ films, even though the optimal MW in the case of 100 nm-sized NPs is less than or equal to 2 kg/mol. Given that it is impossible to use AA acid monomers as building blocks in LbL assembly, one would intuitively expect there to be an optimum MW equal or less than 2 kg/mol for 100 nm-sized PS+ NPs.

Table 1 summarizes the optimum growth behavior for the different NP sizes and PE MWs studied. For both PAA/PS+ composites with either 23 or 44 nm-sized particles (Figs. 6 and 7) and for PEI/PS- thin films with 41 nm-sized particles (Fig. 4), there is an intermediate MW that leads to the fastest LbL growth. However, the growth rate of PEI/PS- multilayers with 26-nm and 100-nm sized particles does not show an optimal MW over the range of MWs considered (Figs. 3 and 5). Consequently, one can conclude that the effect of MW on growth kinetics of PE/NP thin films strongly depends on the specific chemistry of the ingredients as well as on the size of NPs employed. We should also note that the surface charge density of the sulfate-functionalized particles (PS-) used in growth of PEI films varies greatly with particle size while the amidine-charged particles (PS+) have nearly the same charge density for all three particle-sizes, and this may also play a role in the different behavior observed for the two systems. Further, as mentioned in the experimental section, PEIs had greater polydispersity indices compared to the PAAs. This could also contribute to the different growth kinetics seen for the two systems studied. Even though it is beyond the scope of the current study, the polydispersity of the

polymer solutions employed could have a considerable effect on the growth behavior and is worth future investigation.

Table 1. Optimum LbL buildup for different PE/NP composites studied as a function of NP size and MW of PE.

PEI/PS- NPs multilayers		PAA/PS+ NPs multilayers	
NP size	Optimum MW	NP size	Optimum MW
26	Large (750 kg/mol)	23	Intermediate (5 kg/mol)
41	Intermediate (70 kg/mol)	44	Intermediate (5 kg/mol)
100	Large (750 kg/mol)	100	Intermediate (2 and 5 kg/mol)

Chain diffusion, particle and chain redissolution, specific chemistry involved in the complexation of opposite charges, surface overcompensation and interparticle bridging are some of the major factors whose relative influence controls the overall LbL growth rate. MW, in particular, affects each of the latter factors in different and even opposite ways. For instance, chain diffusion is enhanced while interparticle bridging is adversely impacted as MW decreases. Our results demonstrate that flipping the sign of the charges borne by PEs and NPs leads to two distinct trends in dependence of LbL growth on MW.

For neutral polymers, the self-diffusivity decreases as the MW increases.[31] Decreasing the MW of the PE at otherwise identical conditions therefore increases the effective chain diffusivity, which tends to increase chain deposition into the film. On the other hand, we speculate that each deposited PE layer bridges the former and subsequent NP deposits. Longer chains can bridge the NPs more easily and the chain entanglement would strengthen such interparticle bridges, boosting the film mechanical integrity. A trade-off between the chain diffusivity and bridging could explain the intermediate optimum MW found for PEI/PS- composites with 41 nm-sized PS- particles, as well as PAA/PS+ LbL films. However, the reverse trend is observed for two of the particle sizes employed in PEI/PS- system (Table 1), where for 26 nm-sized particles, appreciable redissolution appears to control the deposition rate (Fig. 3). During chain deposition, the film surface charges arising from sulfate groups are compensated by the amine groups along PEI chains. The incoming chains generally overcompensate the surface charges, reversing the sign of the surface charge. Longer chains have been shown to lead to greater charge overcompensation.[32] Even though a better charge overcompensation for the PEI with the highest MW can explain the deviation from the observed trend for PAA/PS+ NP system, further detailed experimental techniques are needed to definitively elucidate this observation and better understand the underlying physics. It might be possible, for example, to use confocal laser scanning microscopy or neutron reflectometry to track the diffusion of polymer in the LbL film which could shed light on the reason for different growth behaviors.[33] Also, single-molecule force spectroscopy experiments could be done wherein a polymer chain is detached from the film and the detachment

force profile is measured. This has been proven to be a useful method to determine polymer chain adhesion forces in films.[34]

For larger PS NPs, it is more difficult for PEs to create interparticle bridges and LbL films become unstable in this case. Interparticle bridging becomes even more difficult for shorter PE chains. This might be the reason for larger error bars seen in Fig. 8.

2.2.2. Effect of salinity

Salt screens the electrostatic interactions between charged functional groups and also impacts the PE diffusivity in the multilayer film. The effect of the salinity of the deposition solutions for PAA/PS+ films composed of 44 nm-sized PS+ particles and PAA with MWs of 5 and 240 kg/mol are shown in Figs. 9 and 10, respectively. PS+ NPs with diameter of 44 nm were chosen, as this size was an intermediate nanoparticle size among different PS+ nanoparticle sizes studied. According to Fig. 7, for this nanoparticle size, PAA with MWs of 5 and 240 kg/mol showed the fastest and slowest growth rates, respectively. We therefore chose these MWs to study the effect of salinity for both fast and slow growing films. For the PS+ suspension, even 100 mM salt content did not compromise the suspension stability as verified by dynamic light scattering.

It should be noted that pH of PE and PS solutions were adjusted by the addition of KOH and HCl for different cases studied. This introduced additional K^+ and Cl^- ions to the solutions on top of those introduced by adding KCl. In this section, the term “salinity” refers to the K^+ and/or Cl^- added to the solutions via KCl salt, not including any ions contained in the pH buffer, KOH or HCl. To enhance clarity, the values of ionic strength of the deposition solutions (considering both ions introduced by addition of salt as well as pH buffers) are reported in figure captions. For the case of PS+ NPs, the concentration of ions added to the system for the pH adjustment was far lower than the amount of K^+ and Cl^- ions added to the system to study salinity, so their effect on ionic strength was negligible. For PAAs, however, that was not the case. For the PAAs, the higher the salt concentration (KCl), the greater the concentration of K^- ions needed for pH adjustment. All in all, PAA solutions with higher salt contents needed more ions for pH adjustment too.

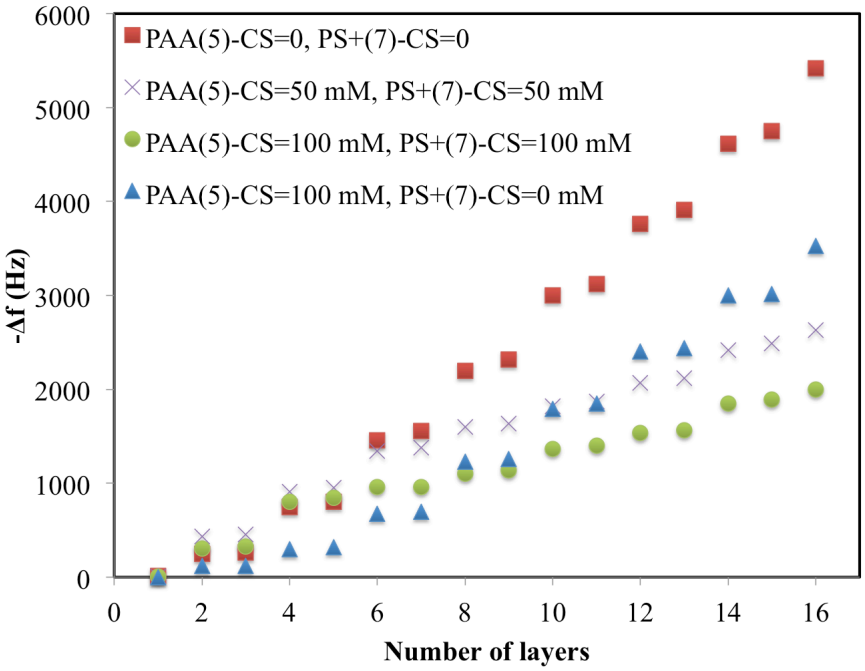

Figure 9. The effect of KCl concentration on growth kinetics of PAA/PS+ multilayers, for PAA with a MW of 5 kg/mol, and 44 nm-sized PS+ particles. Concentration of NPs was 0.1 wt%. The concentrations of salt (CS) in the PAA and PS+ solutions are shown in the legend. The ionic strength was 37, 93, and 147 mM for PAA solutions with salt concentrations of 0, 50, and 100 mM, respectively. For PS+ suspensions however, pH adjustment did not change the ionic strength of the suspensions. Thus, the ionic strength values were the same as salt concentration reported.

As shown in Fig. 9, the addition of KCl to solution of PAA with a MW of 5 kg/mol has a detrimental effect on the buildup of the PAA/PS+ composite film, with the growth rate decreasing when 50 mM salt is added to both PAA and PS+ solutions, and a further decrease when the salt concentration is increased to 100 mM. Also, introducing KCl to the PAA solution only leads to a weaker degradation than when it is added to both solutions. Finally, Fig. 9 also demonstrates that with the addition of KCl, composite films still grow linearly.

The effect of salinity on the growth rate of multilayer films composed of PAA (M_W= 240 kg/mol) and PS+ NPs (44 nm in size) is indicated in Fig. 10.

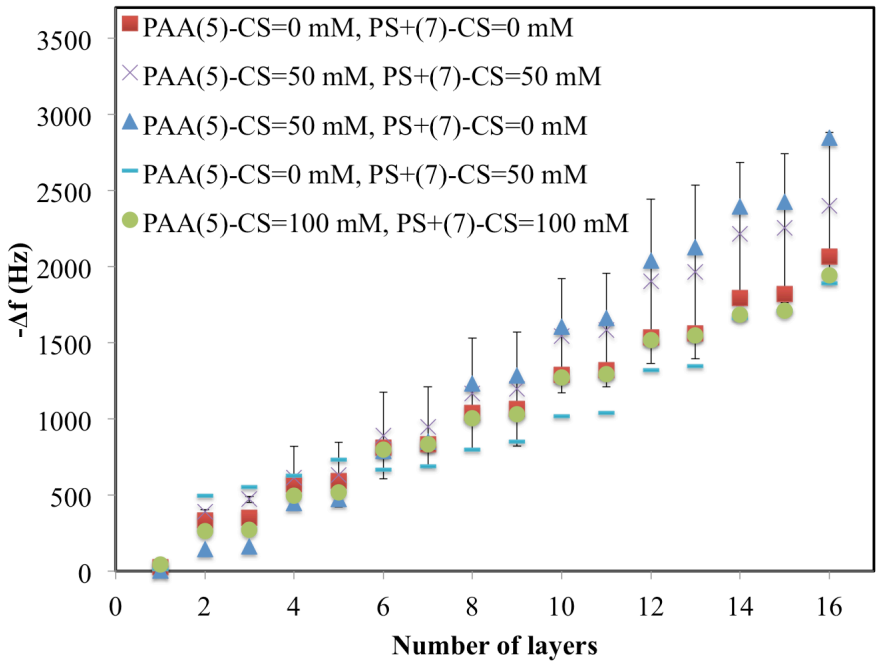

Figure 10. The same as Fig. 9 except for PAA with a MW of 240 kg/mol. The concentration of PS+ NPs was set to 0.1 wt%. The ionic strength for PS+ suspensions with salt content of 0, 50, and 100 mM was 0, 50, and 100 mM, respectively. Also, the ionic strength for PE solutions with salt concentrations of 0, 50, and 100 mM was 34, 92, 149 mM, respectively.

Based on Fig. 10, for PAA with a MW of 240 kg/mol, the addition of KCl to both PAA and PS+ solutions or to PAA solution alone boosts the LbL growth kinetics. However, the LbL growth is slightly degraded when KCl is only introduced into the PS+ suspension.

Figure 10 also illustrates that increasing the salt concentration from 50 mM to 100 mM decreases the growth rate of the PAA/PS+ composite film, for PAA with a MW of 240 kg/mol. Comparing Figs. 9 and 10, one can clearly observe that salinity of the medium has a stronger effect on frequency shifts of PAA/PS+ films for the smaller MW of 5 kg/mol than for MW of 240 kg/mol. 240 kg/mol was the largest MW of PAA investigated in this study because for much higher MW values, the higher viscosity made it practically impossible to study their film growth kinetics.

Although in the work presented here the PEs interact with surface functionalized NPs rather than with other polymers, as is the case for ordinary PE/PE deposition, the key interactions in both cases are electrostatic, and can be screened by mobile salt ions. In both cases, increasing the ionic strength decreases the thermodynamic driving force for complexation of PE and NP functional groups, and enhances the diffusivity of PE chains inside the films, a competition that has been shown to affect PE/PE multilayer formation profoundly.[22] Which of these two factors is dominant thus determines whether the film growth is enhanced or degraded by the addition of salt. The relative importance of these two factors in the present study is affected by the MW of the PE. The diffusivity of the PE with

low MW is already so high that salt should have only a marginal effect on chain diffusivity. Consequently, for low MW PEs, the reduction of the driving force is the dominant factor, which progressively slows down the growth kinetics of low MW PAA/PS+ NP composites as the salt concentration increases (Fig. 9). Interestingly, adding salt only during PAA deposition (while using a salt free NP suspension) leads to an intermediate growth rate.

For the PE with a higher MW, the boost in diffusivity due to the addition of salt apparently outweighs the reduced electrostatic attraction between the oppositely charged components, for salt concentrations up to 50 mM KCl, leading to a boost to LbL growth rate visible in Fig. 10. However, a further increase of salt concentration from 50 to 100 mM and the consequent reduction in the electrostatic driving force degrade the growth kinetics of PAA/PS+ composite. Unlike PEs, the deposition of NPs in Fig. 10 is weakly affected by KCl whereas changing the salt concentration in the PAA solution while holding that of the NP dispersion fixed appreciably alters the growth kinetics. In contrast with spherical NPs, PE chain conformation, thermodynamics and diffusivity are all drastically altered by the ionic strength of the media and LbL growth rate is thus more sensitive to salinity of the PAA solution than to that of the NP dispersion.

2.3. Film characterization

2.3.1. Atomic force microscopy study

To study the surface morphology, the PEI/PS- composites with 41 nm-sized PS- particles were selected. These composites are similar to most of the cases studied in that the intermediate value of MW led to the fastest growth rate (Fig. 4). Other than ions added to the solutions for pH adjustment, no extra salt ions were added to the either of the ingredients for the LbL buildup. Further, PEI and PS- solutions were deposited at pH values of 9.9 and 7, respectively. Figure 11 depicts surface characteristics of composites with different PEI MWs. Instead of performing localized AFM on a very small area, which is a common practice in the literature, a larger area (30 μm×30 μm) was studied to obtain a more representative assessment of the surface morphology. As mentioned previously, 8 different areas of each sample were imaged, but a single image most typical in the range of roughness for each sample is shown in Fig. 11. The inset for each AFM image in Fig. 11 is in fact the same image as in the corresponding main figure, except with the color scale bar fixed to a range of 700 nm, while in the main figures the scale bars are adjusted to keep the contrast fixed. Thus, the insets allow one to compare the uniformity of roughness from sample to sample, with a uniform color and darkness indicating a film with relatively uniform roughness. The thin films, comprising a few layers, are uniformly dark in the insets because there can be little height variation on a scale of 700 nm when the films are much thinner than 700 nm. The main figures, with variable scale bars and fixed contrast, allow one to observe the surface topology, and the variation in height can be assessed for each figure from the corresponding color scale bar.

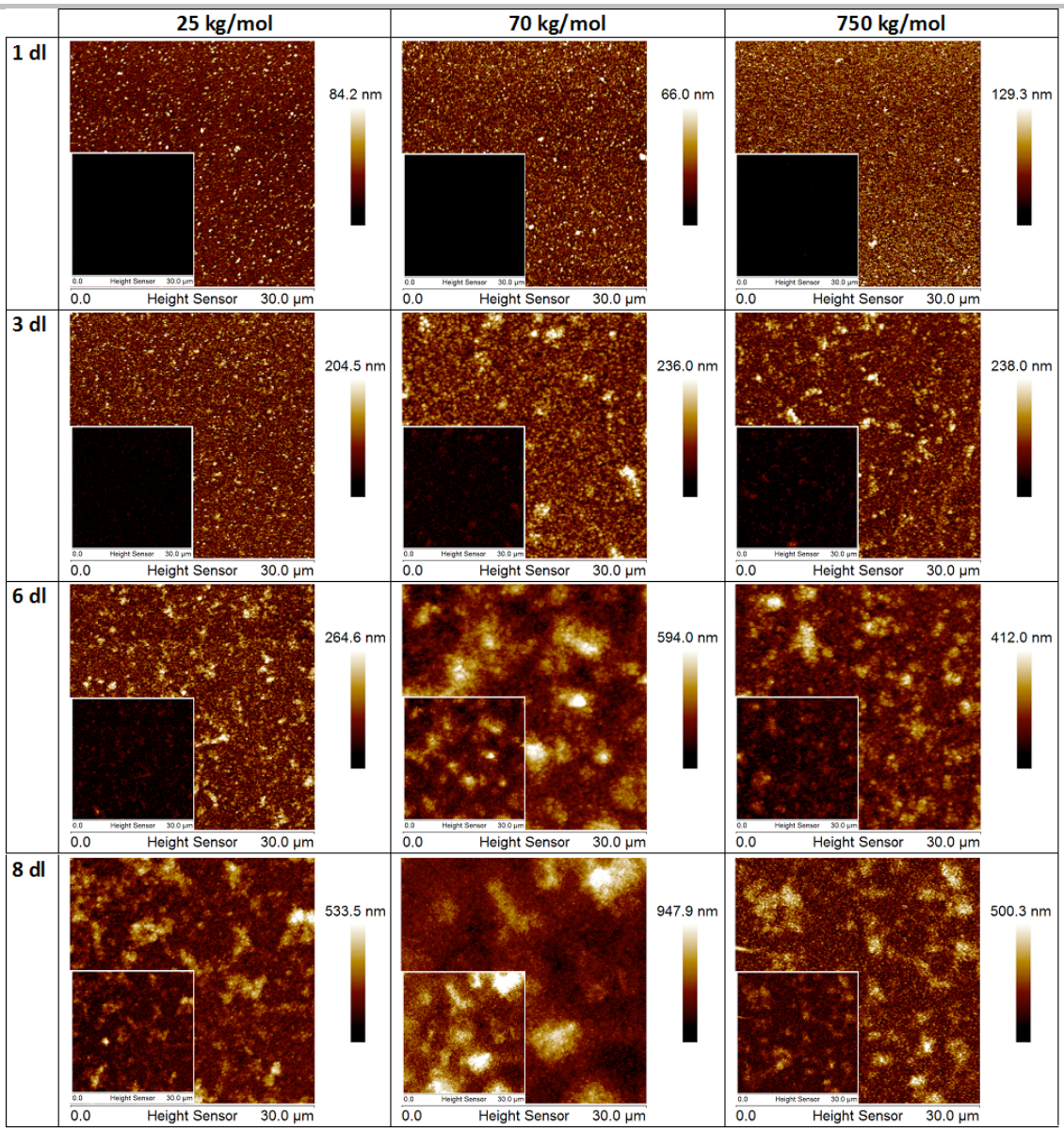

Figure 11. AFM images of PEI/PS- composites with 41 nm-sized PS- particles and different MWs of PEI for different numbers of layers. All the images were obtained once PS- NPs are deposited for 1st, 3rd, 6th, and 8th bilayers. The pH values for the NP and PEI deposition steps were 7, and 9.9, respectively. No salt ions were added for the growth of these films except for the ions introduced to the system to adjust the pH. The scale bars for the main images are also shown. The insets show the corresponding images rendered using a fixed 700 nm scale bar to allow comparison of film height uniformity on an absolute scale.

As can be seen in Fig. 11, surface roughness during the growth of LbL films increases dramatically. This trend is seen for all PEIs with different MWs. Some studies have mentioned that LbL growth under pH-amplified condition, i.e. deposition of film ingredients at different pH values, could lead to rougher surfaces.[18] We tested the effect of pH-amplified deposition on the surface morphology of LbL films by first depositing 8 bilayers of PEI and PS- at pH values of 9.9 and 7, respectively, and contrasting these results with those obtained by depositing the same number of layers of PEI and PS- solutions both at a pH of 7. Root-mean-squared (RMS) roughness values of film surface were determined by examining

the results with Nanoscope Analysis software (Bruker Nano Inc.). AFM micrographs, in the supporting information (Fig. S5), show that in the latter case (equal pH), the rms surface roughness is around 32 % smaller than in the former (unequal pH). However, since the two cases produced differing total film thickness, and roughness generally increases with thickness (Fig. 11), rather than comparing the surface roughness for a fixed number of layers, the roughness-to-thickness ratio is a better basis for comparison, since normally one wants to achieve a layer of a given thickness. Due to much slower growth of PEI/PS- composite when both PEI and PS- solutions are deposited at a pH value of 7, in this case the ratio of roughness to thickness is around 30 % higher than in the pH amplified deposition condition. So, it seems that the amplification of LbL growth by using different pH values for different layers does not increase roughness, at least when roughness is normalized by film thickness. Another possible reason for the high surface roughness could be an uneven distribution of surface charge on the crystal surface, despite the fact that we were careful to be consistent when treating the substrates with piranha solution.

Figure 12 depicts the variation of both absolute roughness (shown in the inset) and roughness normalized by the film thickness for PEI/PS- thin films with different PEI MWs. Average film thicknesses of PEI/PS- films composed of PEI with MWs of 25, 70, and 750 kg/mol were estimated to be 330, 825, and 270 nm, respectively. These estimations were obtained by converting the frequency shift (data in Fig. 4) of the QCM measurements to mass per unit area using the Sauerbrey equation (Eq. (1) shown in the experimental section). Knowing the mass per unit area and the density of film ingredients, one can estimate average film thickness. Because of the much greater mass deposition of NPs than of PE's, the density of the PS (1.05 gm/cm^3) is used to convert the mass of film into thickness. This way, the effect of the small density difference between the PS and the PE's is neglected. This makes calculations much easier, and generates minimal error (~0.3% in the worst case) in the final results.

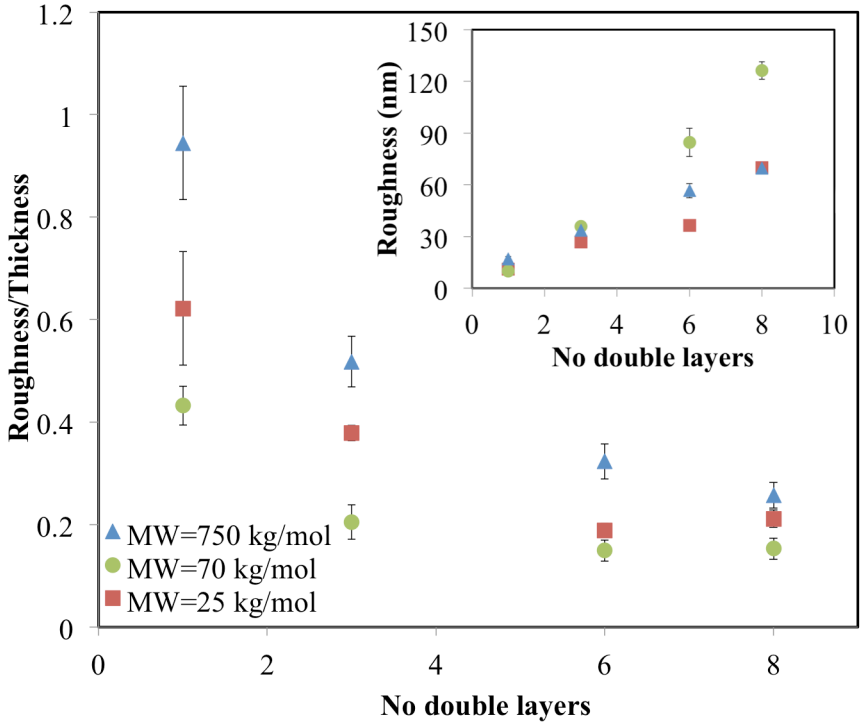

Figure 12. Ratio of roughness to thickness, extracted from AFM images, for the PEI/PS- multilayers depicted in Fig. 11. The inset shows the variation of absolute roughness. For some data points, the error bar is too small to be visible.

Figure 12 shows that regardless of the MW of the PEI, as more layers are deposited onto the films, the ratio of roughness to thickness decreases while the absolute roughness increases. Further, Fig. 12 shows that PEI with intermediate MW has the least roughness to thickness ratio, perhaps due to the fast growth of its thickness. As can be seen in the inset to Fig. 12, LbL films composed of PEI with MWs of 25 and 750 kg/mol have comparable roughness values. Interestingly, these films had a similar rate of multilayer buildup (Fig. 4).

2.3.2. Scanning electron microscopy study

2.3.2.1. Effect of molecular weight

Figure 13 shows SEM micrographs of the surfaces of LbL films with different molecular weights of PEI, grown with the same materials and under the same conditions as for the AFM images in Fig. 11. At least five different regions of the samples were randomly selected to obtain the micrographs with magnifications of 400. Those chosen for Fig. 13 represent the typical features observed in the images. For micrographs with a magnification of 80,000, however, only three different parts of the samples were imaged, since different micrographs looked very similar to each other at this magnification.

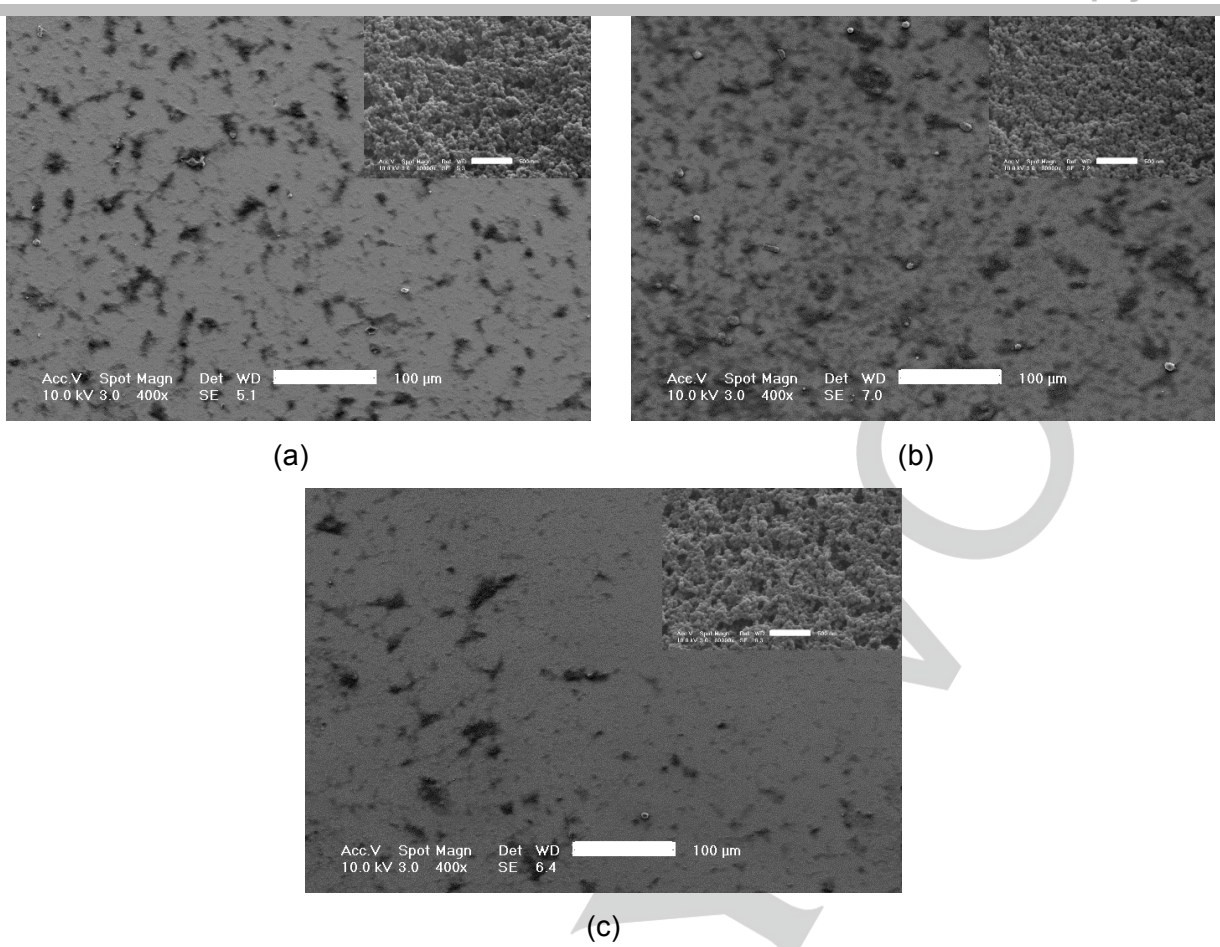

Figure 13. Surface morphology of LbL films composed of 8 double layers of PEI and PS-, with the same materials and the same conditions as for Fig. 11, with PEI MWs of 25 kg/mol (a), 70 kg/mol (b), and 750 kg/mol (c). The main figures have a magnification of 400 while the insets have a magnification of 80,000. The scale bars represent a length of 100 µm in the main figures, while those of insets indicate a length of 500 nm.

Figure 13 shows that the PEI/PS- multilayer film composed of PEI with MW of 70 kg/mol has a more heterogeneous surface than do the films for the other two molecular weights studied, which is consistent with the AFM results.

2.3.2.2. Thick film growth

PEI with a MW of 70 kg/mol and 41 nm sized PS- particles led to the thickest LbL film among different PEI/PS- composites studied in the previous sections. Thus, for this multilayer film, the LbL growth was continued until 59 double layers of PEI/PS- NPs were deposited on the glass substrate. Then, the surface morphology and thickness of the film were studied. Figure 14 depicts the characteristics of such composite obtained by SEM.

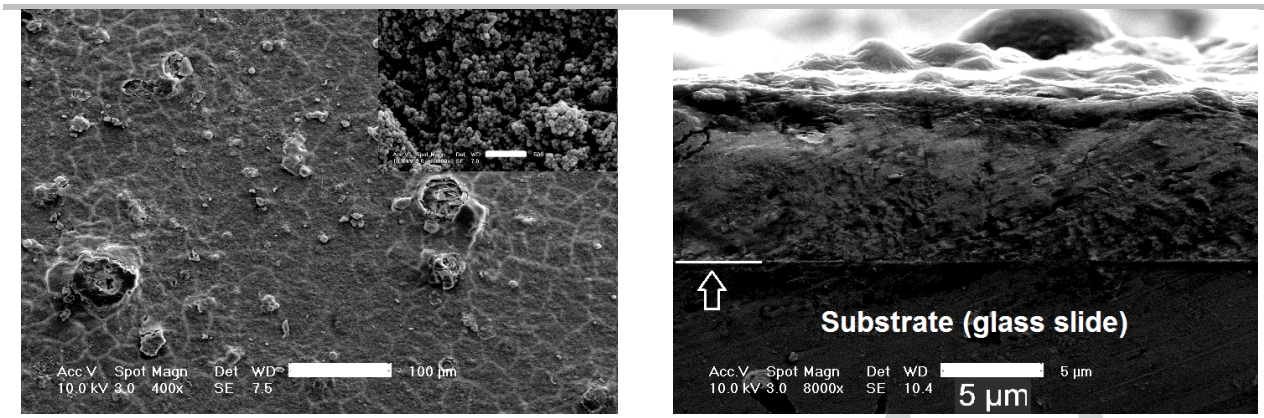

(a) (b)

Figure 14. Characteristics of LbL film composed of 59 double layers of PEI and PS- NPs, with PEI MW of 70 kg/mol. PEI and PS- solutions were deposited at pH values of 9.9 and 7, respectively. No salt was used in either of the film ingredients except for the addition of HCl or KOH for pH adjustment. (a) Surface of the film with a magnification of 400 in the main figure and 80,000 in the inset. The scale bars show a length of 100 µm for the main figure and 500 nm for the inset. (b) Cross sectional view of the film with a magnification of 8,000. The arrow indicates the interface between the substrate and the film.

As can be seen in the surface micrograph (Fig. 14 (a)), the glass slide is completely covered by the film ingredients. There were some cracks and uneven features noticeable on the surface of the film however. Comparing the insets of Fig. 13 and Fig. 14 (a), we see more dark regions in the latter, possibly indicating that the films are more disorganized and particles are more aggregated for the thicker film shown in Fig. 14 (a). Moreover, Fig. 14 (b) shows that a relatively thick film with thickness of few microns is deposited on the substrate. Film thickness was not uniform throughout the cross section and could have drastic variations. To be able to do SEM on the film cross section, the substrate was broken. As can be seen in Fig. 14 (b), film cross section is slightly scratched as a result of breaking the glass slide.

3. Concluding remarks and future work

We studied the effect of molecular weight (MW) of polyelectrolytes (PEs), type and charge of PE, nanoparticle size, pH, and salinity on the growth kinetics of polyelectrolyte (PE)/organic nanoparticle (NP) multilayer films. First, we found that we could not deposit oppositely charged NPs alternately on top of each other in a manner that could survive rinsing steps, unless there are intervening polyelectrolyte layers. This shows that the polyelectrolyte and its binding and bridging of NPs is an essential mechanism for LbL film growth involving NPs. We showed that for both cationic poly(ethyleneimine) (PEI) deposited alternately with anionic polystyrene (PS-) NPs and for anionic poly(acrylic acid) (PAA) deposited alternately with cationic PS (PS+) NPs, an intermediate value of MW can (with some exceptions) lead to the fastest film buildup. This behavior can be explained as a trade-

off between faster diffusivity for smaller chains during the deposition step at the expense of weaker adhesion and wash-off of particles during the deposition or rinse step when the MW becomes too low. However, for films composed of PEI with 26 or 100 nm sized particles, the PEI with the highest MW led to the thickest film.

The pH of PEI and PS- solutions had a dramatic influence on the LbL growth; in general, reducing the charge on the PEI by depositing it at higher pH caused greater deposition of PEI and of subsequent layers of PEI and NPs. Especially fast film growth was obtained by depositing PEI at pH = 9.9 and oppositely charged PS- NPs at 7.0. We showed that salinity affects the growth kinetics of LbL films differently depending on MW of the PE. For low MW PEs, increasing the salt concentration decreased the film growth rate monotonically, while for larger PE MW, addition of salt first improved and then degraded the multilayer buildup.

Some of these trends, especially the effects of pH and PE molecular weight, and to some extent the effect of salinity, can be understood qualitatively. But even the general trends observed were defied for some particle sizes, depending on the particular PE. Even when the expected trend was followed, for example the non-monotonic dependence of growth rate on PE molecular weight, the value of the optimal molecular weight varied greatly (more than an order of magnitude) from PEI to PAA, for no reason we could determine. Hence, while some qualitative trends are now evident and explicable, even semi-quantitative predictions are not yet in sight, and there are polymer-specific exceptions to even the qualitative trends.

Clearly, much progress is still needed to develop an improved qualitative and quantitative understanding of LbL deposition of PEs and NPs. In addition to further systematic LbL growth experiments such as those performed here, more detailed microscope experiments could be very helpful, such as AFM studies of binding and adhesion forces between individual NPs and PEs, direct measurements of PE and NP diffusion in the film, fluorescence resonance energy transfer (FRET) measurements of binding and unbinding events, and other direct measurements of molecular structures and transitions. Applications of these methods to drug delivery and other applications can be pursued, based in part on the film-growth optimization results and methods presented here.

Experimental section

Materials

PEI and PAA with different MWs were employed as the polycation and polyanion, respectively. Branched PEI with MWs of 750 (Polydispersity index (PDI): 12.5) and 25 kg/mol (PDI: 2.5) were purchased from Sigma-Aldrich (St. Louis, MO). Branched PEI with a MW of 70 kg/mol (PDI: 13) and PAA with MWs of 2, 5 and 30 kg/mol (PDI for these polymers: 2.4) were purchased from Polysciences (Warrington, PA). PAA with a MW of 240 kg/mol was obtained from Acros Organics (Belgium). The PDIs were obtained from the manufacturers.[35] Negatively charged PS (PS-) NPs bearing sulfate functional groups with particle sizes (diameters) of 26±3, 41±6, 100±8 nm as well as positively charged PS (PS+) NPs with amidine functionalization and particle sizes of 23±5, 44±6, 100±9 nm were

purchased from Life Technologies (Eugene, OR). The sulfate-functionalized NPs (PS-) with sizes of 26, 41, and 100 nm had highly varying surface charge densities of 3.4, 0.6, and 0.2 μC/cm^2, respectively. On the other hand, the NPs bearing amidine functionalization (PS+) with sizes of 23, 44, and 100 nm had nearly the same surface charge densities of 3.0, 3.4, and 3.2 μC/cm^2, respectively. The surface charge densities and particle sizes were obtained from the manufacturer.[35] KCl was obtained from Sigma Aldrich to study the effect of salinity on the LbL growth. All other materials were purchased from Sigma Aldrich. No additional purifications were performed on the materials.

Quartz crystal microbalance measurements

The growth of PE/NP multilayers deposited on quartz crystals was monitored in the dry condition with a quartz crystal microbalance (QCM-200, Stanford Research Systems Inc., Sunnyvale, CA). Chrome/gold coated quartz crystals were obtained from Stanford Research Systems and had a resonance frequency of around 5 MHz. Initially, crystals were treated using piranha solution (a mixture of sulfuric acid and 30 % hydrogen peroxide at 3 to 1 volumetric ratio) for 2.5 minutes. Note that piranha solution is very reactive and dangerous and considerable care should be taken when handling it. Piranha treatment not only cleans the substrate, but it also makes it negatively charged. Such a negatively charged substrate is needed for the subsequent PE deposition step. Next, the crystals were rinsed thoroughly with DI water and dried with airflow. HPLC water (Fisher Scientific, Waltham, MA) was used for preparing PE or PS solutions. PE solutions employed in this research all have the same monomer concentration of 0.23 M. Also, PS suspensions were used at a concentration of 0.1 wt% unless specified otherwise. PS suspensions were sonicated with a probe sonicator (Ultrasonic Processor, Cole-Parmer Inc., Vernon Hills, IL) for 33 seconds prior to use in order to avoid agglomeration of NPs. To adjust the pH value of the PE/PS solutions, HCl and KOH were used and pH values were measured with an Orion 3Star Benchtop pH and conductivity meter (Thermo Scientific). In each plot in the results and discussion section, the pH for each solution used during multilayer growth is expressed in parentheses. The pH of deposition solutions was adjusted at the beginning of the LbL growth experiments. We found that for rinsing waters and NP suspensions, the pH drifts over time. For the case of rinsing water and NP suspension at a pH value of 7, pH drift was not significant and was typically below 0.5 units. However, for rinsing water with pH = 9.9, the variation in pH could be larger (even more than 1 pH unit). A similar pH variation during LbL growth has been reported by Peng et al.[24] In the supporting information (Fig. S3), we have compared the effect of pH drift on LbL growth. We believe that such a drift does not have a significant influence on the trend of the results as all of the experiments were performed in relatively similar condition and time duration. For the PE solution, pH drift was not found to be an issue, as the pH was stable over several days.

To commence the LbL growth, the PE solution was poured onto the crystal surface and was left there for 15 minutes unless specified otherwise. Subsequently, using DI water with the pH of the

deposition solution, the crystal was rinsed to remove excess PE chains that are not attached to the surface electrostatically. Next, the crystal was dried with a mild airflow. Afterwards, the variation in vibration frequency was recorded using the QCM. Subsequently, the above-mentioned procedure was repeated for the PS suspension to deposit a PS layer on top of the deposited PE layer. The deposition of PE/PS layers was continued until 8 bilayers were grown on the quartz substrate.

As mentioned before, the resonance frequency shifts of the chrome/gold crystal oscillator were recorded after each deposition step in each experiment. According to the Sauerbrey equation for rigid films,[24, 36, 37] the deposited mass per unit area (or thickness) is linearly related to the shift in resonance frequency as shown in Eq. (1).

$$\Delta f = -C(\Delta m) \quad (1)$$

Where Δf is variation of vibration frequency of the QCM crystal, Δm represents the deposited mass per unit area, and *C* is crystal's sensitivity factor which is 56.6 Hz.cm^2/μg for the chrome/gold-coated quartz crystals as reported by the manufacturer.[37]

Prior to the growth of a PAA/PS+ composite, a layer of PEI with a MW of 750 kg/mol and pH of 7 was deposited onto the substrate as the precursor, or primer layer. However, PEI/PS- multilayers were directly grown on the crystal without needing a precursor layer. All the experiments were performed at room temperature of 22±3. It should be noted that in all the plots shown in the results and discussion section, odd-numbered and even-numbered steps represent PE and PS depositions, respectively.

Growing thick multilayer films

To grow films of several LBL assembled PE/PS double layers, an LbL robot (StratoSequence, nanoStrata Inc., Tallahassee, Fl) was used. The films were grown by dipping a microscope glass slide (Fisher Scientific, Waltham, MA) into PE/PS solutions for 10 minutes. For QCM experiments, a deposition time of 15 minutes was used. We studied the effect of deposition time on LbL growth using QCM and found that there is negligible variation in film growth between 10 and 15 minutes deposition times (results shown in the supporting information, Fig. S1). Thus, we chose a 10-minute deposition time for growing very thick films with the robot to reduce LBL buildup time while ensuring maximum film growth. After each deposition step, the glass slides were dipped successively into two beakers containing DI water with the pH set the same as in the preceding deposition solution. Subsequent to the rinsing steps, the film was blown dry with a flow of air for 3 minutes. The film buildup was continued until 59 double layers of PE/PS were deposited onto the surface. The glass slide was treated with piranha solution prior to the film growth. The amount of each dipping solution was constantly monitored to ensure that the solution volume remained at nearly 120 ml throughout the experiments. The PS suspension was sonicated each time considerable agglomeration of NPs was seen due to dipping of the glass slide and possible complexation formation of free NPs with film ingredients. Fresh particle suspensions used for thick multilayer growth looked clear. When the PS suspension seemed too

cloudy and contaminated by multiple dipping steps, the entire suspension was changed to a fresh one. For the PE solution, however, no noticeable change was observable in solution quality after the dipping steps. Nevertheless, as a precaution, the PE solution was changed after every 20-bilayer buildup, or so. Further, the rinsing waters were changed with fresh ones after every 4-double layer growth.

Atomic force microscopy studies

An atomic force microscope (Dimension Icon, Bruker Nano Inc., Santa Barbara, CA) was employed to study the surface morphology of the films during LbL growth. AFM tips (OTESPA, Bruker Nano Inc., Santa Barbara, CA) with a nominal resonant frequency of 300 kHz, spring constant of 26 N/m, and nominal tip radius of 7 nm were used. AFM measurements were carried out with a scan rate of 1 Hz and in tapping mode.

In each LbL experiment, a fresh quartz crystal was employed. It should be noted that the surface of the LbL films was composed of some rough and smooth regions. As more layers were deposited onto the surface, the proportion of rougher areas increased. A sample photo taken by the optical microscope of AFM is shown in the supporting information (Fig. S6). The roughness of these areas could reach as high as a couple of microns for films with 8 PE/NP double layers, which was beyond the AFM measurable range. Thus, we did AFM analysis on relatively smooth areas only. For each sample, 8 different smooth areas were randomly selected for doing AFM and roughness values were averaged to increase measurement accuracy. We did not try to measure precisely the fraction of “smooth” surface present, but did notice that it decreased with increasing numbers of layers, from perhaps 60% “smooth” by the end of first double layer growth to around 20% “smooth” after deposition of 8 double layers.

Scanning electron microscopy studies

The surface of LbL films was imaged with a FEI XL30FEG scanning electron microscope, with an accelerating voltage of 10 kV, and magnifications of 400 and 80,000. A magnification of 8,000 was chosen to obtain SEM cross section micrographs. As investigated LbL films were not conductive, prior to doing SEM, their surfaces were coated with a thin layer of gold.

Error analysis

The standard error for each parameter studied is calculated via Eq. (2). These parameters include frequency shift of QCM crystal (Δf), thickness (t) (determined using the Sauerbrey equation (Eq. 1) and converting the mass per unit area into thickness), and rms roughness values (R) obtained from AFM measurements.

$$\delta(\mathrm{x}) = \sqrt{\frac{\sum_{i=1}^{N}(x_i - \bar{\mathrm{x}})^2}{N(N-1)}} \quad (2)$$

Where δ is standard error, x is each parameter mentioned above, $\bar{x}$ represents average value of x, and N is the number of replicate experiments done to assess the reproducibility of the results. For determining standard error in frequency shift or thickness, two or three replicate tests were performed for a few of the experiments. Due to time-consuming nature of LbL growth tests, it was practically impossible to repeat all the results reported in this article, and so the error bars given in some of the figures can be taken to be representative. To determine the roughness values, 8 different areas of film were tested to ensure accuracy. The standard errors in our LbL growth measurements based on variation of frequency shift were typically below ~15 %, as determined by replicate runs. The errors could be attributed mainly to small variations in properties of initial layers that are propagated and amplified in subsequently deposited layers. When salt was added to the solutions, the standard error could reach as high as 30 %. Increasing ionic strength is known to reduce the stability of multilayer films[27] and that might have caused the relatively higher error values in these cases.

The standard errors in determining thickness and rms surface roughness of LbL films were generally less than 15 and 10%, respectively. Knowing the errors associated with thickness (t) and rms roughness (R), one can determine the error of the ratio of roughness to thickness using Eq. (3), which is a standard formula for propagation of errors. The calculated error was below 18 % for the worst case studied.

$$\delta\left(\frac{\mathrm{R}}{t}\right) = \frac{\mathrm{R}}{t} \times \sqrt{\left(\frac{\delta(\mathrm{t})}{t}\right)^2 + \left(\frac{\delta(\mathrm{R})}{R}\right)^2} \quad (3)$$

We also carried out a number of LbL deposition experiments involving no polyelectrolytes, but only PS NPs, with opposite charges in alternating layers, the results of which were entirely irreproducible. Insufficient contact area between rigid spherical PS NPs is presumably to blame for the low inter-particle cohesion that compromises the integrity of the whole film. Whatever NPs managed to be deposited were likely washed off during the rinsing steps. Nonetheless, fairly reproducible growth kinetic data (with errors discussed above) were obtained upon replacing one of the two oppositely charged NP solutions with a like-charged PE solution. PEs seem to act as a glue between the PS NPs, stabilizing the resultant composites.

Acknowledgments

The authors would like to thank Prof. Nicholas A. Kotov for providing quartz crystal microbalance, and layer-by-layer assembly robot, and Prof. Steven Schwendeman, and Douglas Montjoy for fruitful discussions. They would like to express gratitude to Dr. Kai Sun and Dr. Haiping Sun from Michigan Center for Materials Characterization for their assistance with AFM and SEM characterization. R.G.L. gratefully acknowledges the support of the National Science Foundation, under grant DMR 1403335. Any opinions, findings, and conclusions or recommendations expressed in this material are those of the authors and do not necessarily reflect the views of the National Science Foundation (NSF). M.M. is a Howard Hughes Medical Institute International Student Research fellow, who is grateful for this support. Moreover, we are grateful for the support provided by Paul R. Lichter, M.D. Research Discovery Fund.

Keywords: Growth kinetics, layer-by-layer (LbL) assembly, polyelectrolytes (PEs), nanoparticles (NPs), molecular weight (MW), salt effect, thin films.

[1] I. Tokarev, S. Minko, *Soft Matter* **2009**, 5, 511-524.

[2] B. K. Kayaoglu, İ. Gocek, H. Kizil, L. Trabzon, *Journal of Textiles and Engineer* **2012**, 19, 39-47.

[3] M. Rahman, N. Taghavinia, *The European Physical Journal-Applied Physics* **2009**, 48, 10602.

[4] M. M. De Villiers, D. P. Otto, S. J. Strydom, Y. M. Lvov, *Advanced Drug Delivery Reviews* **2011**, 63, 701-715.

[5] R. Kniprath, S. Duhm, H. Glowatzki, N. Koch, S. Rogaschewski, J. Rabe, S. Kirstein, *Langmuir* **2007**, 23, 9860-9865.

[6] J. Borges, J. F. Mano, *Chemical Reviews* **2014**, 114, 8883-8942.

[7] J. P. Chapel, J. F. Berret, *Current Opinion in Colloid & Interface Science* **2012**, 17, 97-105.

[8] R. R. Costa, J. F. Mano, *Chemical Society Reviews* **2014**, 43, 3453-3479.

[9] C. Liang, H. Li, Y. Tao, X. Zhou, Z. Yang, Y. Xiao, F. Li, B. Han, Q. Chen, *Journal of Materials Science: Materials in Medicine* **2012**, 23, 1097-1107.

[10] K. Na, S. Kim, K. Park, K. Kim, D. G. Woo, I. C. Kwon, H. M. Chung, K. H. Park, *Journal of the American Chemical Society* **2007**, 129, 5788-5789.

[11] N. Vrana, O. Erdemli, G. Francius, A. Fahs, M. Rabineau, C. Debry, A. Tezcaner, D. Keskin, P. Lavalle, *Journal of Materials Chemistry B* **2014**, 2, 999-1008.

[12] W. Zhao, J. J. Xu, C. G. Shi, H. Y. Chen, *Langmuir* **2005**, 21, 9630-9634.

[13] J. Ma, P. Cai, W. Qi, D. Kong, H. Wang, *Colloids and Surfaces A: Physicochemical and Engineering Aspects* **2013**, 426, 6-11.

[14] K. R. Knowles, C. C. Hanson, A. L. Fogel, B. Warhol, D. A. Rider, *ACS Applied Materials & Interfaces* **2012**, 4, 3575-3583.

[15] S. T. Dubas, P. Kumlangdudsana, P. Potiyaraj, *Colloids and Surfaces A: Physicochemical and Engineering Aspects* **2006**, 289, 105-109.

[16] S. T. Dubas, S. Wacharanad, P. Potiyaraj, *Colloids and Surfaces A: Physicochemical and Engineering Aspects* **2011**, 380, 25-28.

[17] P. Nestler, M. Paßvogel, C. A. Helm, *Macromolecules* **2013**, 46, 5622-5629.

[18] L. Shen, P. Chaudouet, J. Ji, C. Picart, *Biomacromolecules* **2011**, 12, 1322-1331.

[19] J. Yu, O. Sanyal, A. P. Izbicki, I. Lee, *Macromolecular Rapid Communications* **2015**, 36, 1669-1674.

[20] X. Zan, D. A. Hoagland, T. Wang, B. Peng, Z. Su, *Polymer* **2012**, 53, 5109-5115.

[21] M. Rahman, F. Tajabadi, L. Shooshtari, N. Taghavinia, *ChemPhysChem* **2011**, 12, 966-973.

[22] A. Salehi, P. S. Desai, J. Li, C. A. Steele, R. G. Larson, *Macromolecules* **2015**, 48, 400-409.

[23] P. Bieker, M. Schönhoff, *Macromolecules* **2010**, 43, 5052-5059.

[24] C. Peng, Y. S. Thio, R. A. Gerhardt, H. Ambaye, V. Lauter, *Chemistry of Materials* **2011**, 23, 4548-4556.

[25] S. Ghannoum, Y. Xin, J. Jaber, L. I. Halaoui, *Langmuir* **2003**, 19, 4804-4811.

[26] A. Ostendorf, C. Cramer, G. Decher, M. Schönhoff, *The Journal of Physical Chemistry C* **2015**, 119, 9543-9549.

[27] T. Sennerfors, G. Bogdanovic, F. Tiberg, *Langmuir* **2002**, 18, 6410-6415.

[28] Y. Lvov, K. Ariga, M. Onda, I. Ichinose, T. Kunitake, *Langmuir* **1997**, 13, 6195-6203.

[29] J. Choi, M. F. Rubner, *Macromolecules* **2005**, 38, 116-124.

[30] A. I. Petrov, A. A. Antipov, G. B. Sukhorukov, *Macromolecules* **2003**, 36, 10079-10086.

[31] M. Rubinstein, R. H. Colby, Polymer physics, Oxford University Press **2003**.

[32] Q. Wang, *Macromolecules* **2005**, 38, 8911-8922.

[33] C. Picart, J. Mutterer, L. Richert, Y. Luo, G. Prestwich, P. Schaaf, J. C. Voegel, P. Lavalle, *Proceedings of the National Academy of Sciences* **2002**, 99, 12531-12535.

[34] M. Rief, F. Oesterhelt, B. Heymann, H. E. Gaub, *Science* **1997**, 275, 1295-1297.

[35] *Supplier, private communication* **2016**.

[36] G. Sauerbrey, *Zeitschrift für Physik* **1959**, 155, 206-222.

[37] QCM200 Quartz Crystal Microbalance Digital Controller QCM225, 205 MHz Crystal Oscillator, Stanford Research Systems.

Table of Contents

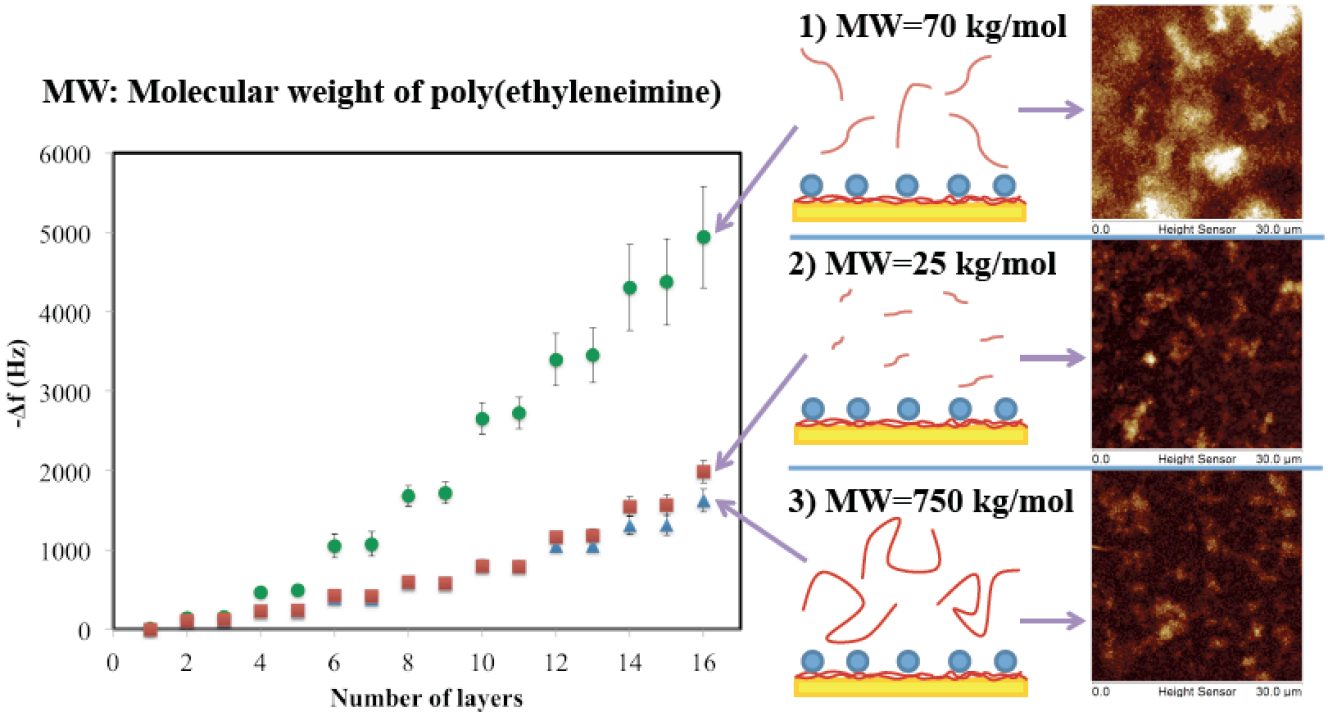

Molecular weight of polyelectrolyte has a considerable effect on layer-by-layer film growth and its surface mophology.